

Autoionizing resonances $4d \rightarrow nl$ in cadmium

J. Jiménez-Mier*

Oak Ridge National Laboratory, Oak Ridge, Tennessee 37831

C. D. Caldwell

University of Central Florida, Orlando, Florida 32816

M. O. Krause

Oak Ridge National Laboratory, Oak Ridge, Tennessee 37831

(Received 3 June 1988)

We measured the relative cross section and angular distribution parameter for $5s$ photoelectron emission in atomic cadmium across the region of the $4d \rightarrow nl$ autoionizing resonances between 11.70 and 18.05 eV. Our results for the oscillator strengths agree with Hartree-Fock calculations, and are higher than the values reported by other experiments. Strong departure from the direct-process value of 2.0 was observed for the angular distribution parameter β , indicating singlet-to-triplet mixing in the wave functions. The mixing varies in the np resonance series, while it remains almost constant throughout the nf series. In the region of the $5p$ resonances there is good agreement with a semiempirical calculation of the asymmetry parameter. A number of double-electron excitations were investigated and the value of β was used to give the correct assignment to a transition at 12.856 eV. A previously unobserved transition corresponding to the promotion of a $4d$ electron to the $5d$ orbit was detected by the change in the value of β .

I. INTRODUCTION

The study of the autoionizing transitions in the cadmium atom enjoys a rich spectroscopic tradition. As long ago as 1933 Beutler¹ measured and analyzed four Rydberg series corresponding to the promotion of one of the $4d$ electrons, culminating in the ${}^2D_{5/2}$ and ${}^2D_{3/2}$ states of the ion. This original work of Beutler was later extended by Berkowitz and Lifshitz² and Garton and Connerade,³ and the total absorption cross section was measured by Marr and Austin.⁴ Above the ${}^2D_{5/2}$ threshold, ionization by removal of one of the $4d$ electrons is the predominant direct process. Yet even this region of the spectrum displays numerous double-electron excitations,⁵ many with large oscillator strengths. Notable among these is the $4d^{10}5s^2 {}^1S_0 - 4d^9[5s5p({}^3P)] {}^2P_{3/2}6s {}^1P_1$ transition at 588 Å, close to the 584-Å He I line.

Because of the large cross section for removal of a d electron, much attention has been devoted to examining Cd photoionization above the $D_{5/2}$ threshold. Photoelectron angular distribution measurements were carried out at the He I line energy by Harrison,⁶ and cadmium was the atom of choice for the first demonstration of alignment in photoionization by Caldwell and Zare.⁷ The angular distribution measurements were later extended over a broad region of the spectrum by Kobrin *et al.*⁸ using synchrotron radiation; alignment measurements were performed over this same region by Kronast, Huster, and Mehlhorn.⁹ Finally, Goodman, Caldwell, and White¹⁰ measured the alignment in the region between the two D thresholds.

Apart from the absorption measurements^{1,3,4} and photoionization measurements,² no detailed study of cadmium photoionization has been carried out in the region of the

spectrum below the $D_{5/2}$ limit, the same region which was explored by Beutler in his early work. Such an analysis should complement the information obtained in electron-impact excitation experiments.¹¹⁻¹⁴ The predominant direct process, the removal of one of the $5s$ electrons, has a very small cross section, so the only readily measurable properties are those associated with the autoionizing transitions. Because the $4d^{10}5s^2$ configuration of the ground state of cadmium is a closed-shell system, calculations can be carried out using existing theoretical techniques, so a direct comparison between theory and experiment is possible.

The excitation spectrum below the $D_{3/2}$ threshold can be separated into three regions according to the energy levels listed in Table I. The first region, from the first ionization potential at 8.99 to 14.5 eV, is characterized by the single direct process corresponding to the removal of one of the $5s$ electrons, dotted with autoionizing transitions corresponding to the promotion of a $4d$ electron to the $5p$ shell, or the simultaneous excitation of both $5s$ electrons.⁵ At 14.5 eV the threshold is reached for production of the excited 2P_j states of the ion. In this second region, presence of ions in these levels in photoelectron spectroscopic measurements indicates configuration in-

TABLE I. Threshold energies in cadmium.

Level	Energy (eV)
$4d^{10}5s^2 S_{1/2}$	8.994
$4d^{10}5p^2 P_{1/2}$	14.466
$4d^{10}5p^2 P_{3/2}$	14.774
$4d^9 5s^2 D_{5/2}$	17.581
$4d^9 5s^2 D_{3/2}$	18.280

teraction involving a mixing of $5p^2$ into the ground state.¹⁵ Above 14.5 eV the d excitation continues until the $D_{5/2}$ threshold is reached at 17.6 eV. The fine-structure splitting between the $D_{5/2}$ state and the $D_{3/2}$ state at 18.3 eV is considerable. The third region covering the interval between these spin-orbit limits is characterized by a number of d excitations based on the $D_{3/2}$ core.³

In this work we will report an extensive analysis of the autoionizing levels from 11.7 to 18.05 eV. We use the technique of electron spectroscopy with synchrotron radiation to analyze electrons corresponding to production of the $^2S_{1/2}$ ground state of the cadmium ion. In this way we examine the coupling of the "bound" state into this single ionic level. We carry out a detailed analysis of the partial cross sections into the various terms and photoelectron angular distributions for a number of the autoionizing transitions. We focus particular attention on the $4d \rightarrow 5p$ resonances. The power of the technique of photoelectron angular distribution measurements is demonstrated when we locate optically allowed excitations by their enhanced effect on this distribution as compared with a change in the cross section.

II. EXPERIMENTAL

The experiment took place at the storage ring Aladdin at the University of Wisconsin Synchrotron Radiation Center. A 4m normal incidence monochromator with a MgF_2 grating (1200 lines/mm) was used to monochromatize the synchrotron radiation. The electron spectrometer has been described previously.^{16,17} It consists of three electrostatic analyzers mounted on a platform that can be rotated in a plane perpendicular to the direction of incidence of the photon beam. In the dipole approximation the intensity distribution of the photoelectrons is given by

$$I_e \propto \frac{d\sigma}{d\Omega} = \frac{\sigma}{4\pi} \left[1 + \frac{\beta}{4} [1 + 3p \cos 2\theta] \right], \quad (1)$$

where p is the synchrotron radiation polarization and θ is the angle between the direction of observation and the major axis of the polarization ellipse. With an analyzer set at the "magic angle" $\theta_m = \frac{1}{2} \cos^{-1} [1/(3p)]$ we measure the relative cross section. With two analyzers placed along the directions of the major and minor axis of the polarization ellipse (0° and 90° , respectively) we obtain the angular distribution parameter β from the relation

$$\beta = \frac{4(R - 1)}{3p(R + 1) - (R - 1)}. \quad (2)$$

Here $R = I(0^\circ)/I(90^\circ)$ is the ratio of intensities at 0° and 90° .

The polarization of the synchrotron radiation, the correction factors due to unequal response of the analyzers, and changes in the source volume seen by the analyzers were obtained from measurements of angular distributions of calibrant gases (Ar, Kr, and Xe) at suitable photon energies. The spectral transmission of the monochromator was obtained by measuring the relative intensity of the $5p$ photoelectrons in Xe and by extrapolating these measurements below 12.13 eV with the aid of

response curves recorded with a sodium salicylate detector and a photomultiplier tube. The measured bandpass of this monochromator was $0.65 \pm 0.07 \text{ \AA}$ at the $5p \rightarrow 8s$ resonance in xenon at 12.575 eV and it was assumed to be constant throughout our energy range. The same resonance in Xe and the analogous resonance in Kr were also used for the energy calibration of the monochromator. The measured polarization was 0.91.

An effusive quasibeam was produced by heating metallic cadmium in a tantalum oven to a temperature of 250° . We estimate that the pressure in the interaction region was in the 10^{-3} – 10^{-4} -Torr range. Constant ionic state (CIS) spectra were recorded by simultaneously scanning the monochromator and the accelerating voltage for the photoelectrons. A typical value of the acceleration applied was -7 V . The stepsize in the CIS mode was either 3, 6, or 12 meV. Photoelectron spectra (PES) were recorded at selected wavelengths to serve as references for the CIS spectra. The relative energy resolution of the electrostatic analyzers was 1%.

III. RESULTS AND DISCUSSION

The photoelectron spectrum of cadmium, taken at a photon energy of 16.64 eV, is presented in Fig. 1. It shows the main $5s$ photoline and the $5p$ satellites. This work concentrated on the study of the behavior of the $5s$ line throughout the region of autoionizing resonances. The intensity ratio of the $5p$ "satellite" lines to the $5s$ was measured at several resonances. It was found that in the $4d \rightarrow 6p$ resonance region the intensity of the $5p$ signal is about 13% of the intensity of the main line. For a photon energy of 17.681 eV, at the $(^2D_{3/2})8p$ resonance, the ratio is 51%, and at 17.874 eV, the peak of the $9p$ resonance, the $5p$ intensity is about 60% of the $5s$ photoline.

A CIS survey spectrum across the autoionizing region studied in this work is shown in Fig. 2. In this case the $^2S_{1/2}$ final ionic state is being monitored. Five series of resonances converging to the $4d^9 5s^2 ^2D_J$ ($J = \frac{3}{2}, \frac{5}{2}$) states of the ion^{3,4} were experimentally resolved. Two of them, the $4d^9 5s^2 (^2D_{5/2})np$ and $4d^9 5s^2 (^2D_{5/2})nf$, converge to

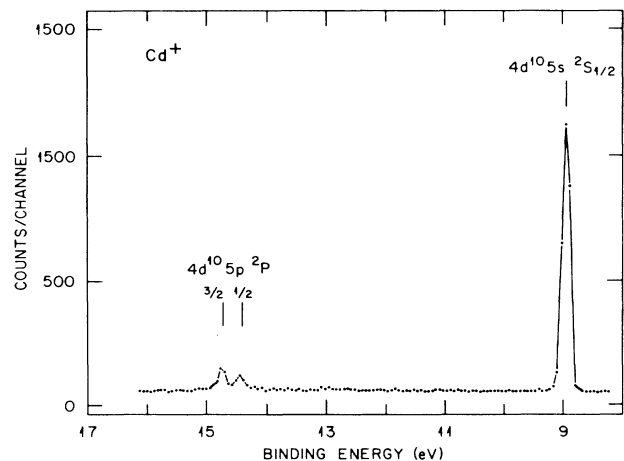


FIG. 1. Photoelectron spectrum of cadmium. The photon energy is 16.64 eV and the analyzer is set at the magic angle.

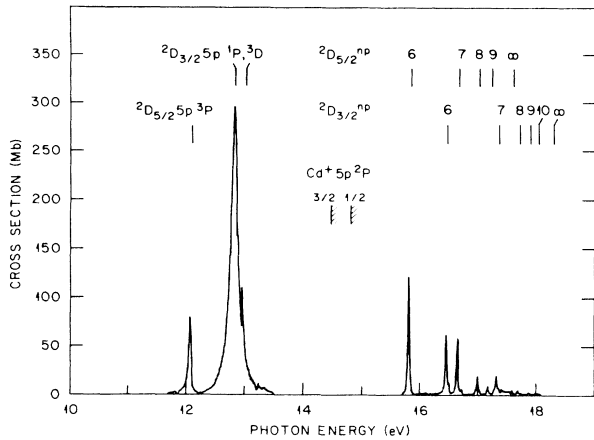


FIG. 2. Survey CIS spectrum of the autoionizing resonances in cadmium. Only the $4d^9 5s^2 2D_{5/2} np$ and $4d^9 5s^2 2D_{3/2} np$ series have been labeled. Also indicated are the $5p^2 P$ thresholds.

the $J = \frac{5}{2}$ state. The other three, namely, the $4d^9 5s^2 (2D_{3/2}) np$, $4d^9 5s^2 (2D_{3/2}) np'$, and $4d^9 5s^2 (2D_{3/2}) nf$ series, converge to the $J = \frac{3}{2}$ state. A list of the measured energies of the autoionizing resonances is presented in Table II. Both LS and Jl labels are used for the $5p$ and $6p$ configurations, while the higher resonances are described only in terms of the more appropriate Jl coupling.^{3,18}

A least-squares procedure was followed to normalize our data to the cross section given by Marr and Austin⁴ in the region of the $5p$ resonances between 12.02 and 12.80 eV. This is a region in which only one exit channel, $4d^9 5s^2 (2S_{1/2}) \epsilon l$, is open. We obtained a cross section of

296.5 Mb at an energy of 12.805 eV, while Marr and Austin reported a peak cross section of 284 Mb. The spectrum in Fig. 2, as well as those in the following figures, are normalized to the 296.5-Mb value, after correcting the recorded spectra for background, storage ring beam current, vapor density, and grating efficiency. Numerical results of the cross section and asymmetry parameter at the autoionizing resonances are shown in Table III. An error of 30% in the cross section values is obtained by combining our experimental errors with the error quoted by Marr and Austin. The errors in the β values range from 0.05 to 0.10 units.

The small cross section for direct photoionization translates into symmetric peak profiles that are nearly Lorentzian, the only exception being the lines in the $4d \rightarrow 5p$ resonance. Because of the finite bandpass of the monochromator the profile of the lines is more of the Voigt type. We can obtain the oscillator strength f of the resonances by calculating the area under the peak and using the expression⁴

$$\int \sigma(\bar{\nu}) d\bar{\nu} = \frac{\pi e^2}{mc^2} f, \quad (3)$$

where $\bar{\nu}$ is the wave number and σ is the cross section. This procedure was followed to determine the oscillator strengths of the Lorentzian-type peaks, and the combined f of the $4d \rightarrow 5p$ resonances. Below we describe the method used to obtain the oscillator strengths of the individual lines in the region of the $4d \rightarrow 5p$ resonances. A comparison of our results with those reported by Marr and Austin⁴ and Berkowitz and Lifshitz² is presented in Table IV. Except for the $2D_{5/2} 5p [3/2]$ resonance, our

TABLE II. Cadmium autoionizing resonances $4d^9 5s^2 (2D_j) nl$.

State		This work ^a	Energy (eV) Absorption ^b	Photoion ^c
$(2D_{5/2}) 5p$	$3P[3/2]$	12.063 ^d	12.062	
$(2D_{3/2}) 5p$	$1P[1/2]$	12.805	12.800	
$(2D_{3/2}) 5p'$	$3D[3/2]$	12.930 ^d	12.939	
$(2D_{5/2}) 6p$	$1P[3/2]$	15.803	15.808	15.8
$(2D_{3/2}) 6p$	$3P[1/2]$	16.453	16.455	16.44
$(2D_{3/2}) 6p'$	$3D[3/2]$	16.499	16.499	16.498
$(2D_{5/2}) 7p$	$[3/2]$	16.642	16.643	16.640
$(2D_{5/2}) 4f$	$[3/2, 1/2]$	16.716	16.716	16.714
$(2D_{5/2}) 8p$	$[3/2]$	16.994	16.994	16.993
$(2D_{5/2}) 5f$	$[3/2, 1/2]$	17.030		17.027
$(2D_{5/2}) 9p$	$[3/2]$	17.179	17.180	17.178
$(2D_{5/2}) 6f$	$[3/2, 1/2]$	17.205	17.203	17.197
$(2D_{5/2}) 10p$	$[3/2]$	17.294	17.290	17.287
$(2D_{3/2}) 7p$	$[1/2]$	17.319	17.324	17.319
$(2D_{3/2}) 8p$	$[1/2]$	17.685	17.687	17.681
$(2D_{3/2}) 5f$	$[3/2]$	17.731	17.730	17.728
$(2D_{3/2}) 9p$	$[1/2]$	17.876	17.873	17.874
$(2D_{3/2}) 6f$	$[3/2]$	17.897		17.897
$(2D_{3/2}) 10p$	$[1/2]$	17.988	17.987	17.985

^aEstimated error is ± 3 meV, photoelectron spectrometry.

^bReference 4.

^cReference 2.

^dTaken at peak of asymmetric line profile.

TABLE III. Cross section σ (in Mb) and photoelectron angular distribution parameter β at the $4d^9 5s^2 ({}^2D_J)nl$ resonances.

n	σ^a	β^b
${}^2D_{3/2}np [1/2]$ series		
5	296.5	1.99
6	63.9	1.01
7	19.4	1.20
8	3.4	1.08
9	1.9	1.19
10	1.3	1.28
${}^2D_{5/2}np [3/2]$ series		
5	80.3	-0.15
6	121.7	1.49
7	56.1	1.95
8	18.6	1.58
9	7.9	1.19
10	6.1	1.01
${}^2D_{3/2}np' [3/2]$ series		
5	111.2 ^c	1.80
6	10.2	1.25
${}^2D_{5/2}nf [3/2, 1/2]$ series		
4	4.6	1.74
5	3.9	1.88
6	1.8	1.36
${}^2D_{3/2}nf [3/2]$		
4	1.8	1.77
5	1.2	1.76
6	0.9	1.72

^aEstimated error in the absolute cross section is 30%.

^bError = ± 0.05 .

^cPeak value includes contribution from the $5p[1/2]$ resonance.

values are consistently higher than those of the other experiments, but they are in very good agreement with the Hartree-Fock calculation of Wilson.²⁰ It should be noted that our values pertain to the decay into the $4d^{10}4s ({}^2S_{1/2})\epsilon l$ channel only, and do not include contributions due to the $5p$ satellite channels accessible at energies above about 14.5 eV. By contrast, the measurements of Refs. 2 and 4 would comprise all exit channel contributions. The measured widths of the autoionizing resonances are given in Table V. These widths are corrected for the width (bandpass) of the incident radiation.

Across the resonances there are deviations from the direct photoionization value of $\beta=2$. This has been explained by Dill¹⁹ in terms of the angular momentum transfer formalism. In the case of an s photoelectron the angular distribution parameter can be written as

$$\beta = \frac{2|D_1|^2 - |D_3|^2}{|D_1|^2 + |D_3|^2}, \quad (4)$$

where D_1 and D_3 are the probability amplitudes for transitions to the singlet and triplet continua, respectively. If there is just coupling to the singlet continuum (parity favored), then $D_3=0$ and the asymmetry parameter is equal to 2. The other extreme case occurs if the triplet continuum is the only continuum, in which case $D_1=0$ and $\beta=-1$. A measure of the coupling strength with the triplet continuum is thus given by the departure of β from the value of 2. A detailed discussion of the features seen in the survey spectrum will be given in the following.

A. $4d^9 5s^2 5p$ resonances

In Fig. 3 we present the results obtained in the region of the $5p$ resonances. The lower panel gives the total cross section, and the upper panel gives the β values.

TABLE IV. Oscillator strengths of cadmium autoionizing resonances.

Peak	This work ^a	Oscillator strength		
		Absorption ^b	Photoion ^c	Theory ^d
${}^2D_{5/2}5p [3/2]$	0.053(1)	0.070	0.041	0.080
${}^2D_{3/2}5p [1/2]$	0.56(1)	0.53	0.24	0.518
${}^2D_{3/2}5p' [3/2]$	0.0010(5) ^e	0.0004		0.001
${}^2D_{5/2}6p [3/2]$	0.036(1)	0.022	0.017	0.031
${}^2D_{3/2}6p [1/2]$	0.021(1)	0.0077	0.009	0.022
${}^2D_{3/2}6p' [3/2]$	0.0010(5)	0.001		0.003
${}^2D_{5/2}7p [3/2]$	0.018(1)	0.006	0.005	
${}^2D_{5/2}4f [3/2, 1/2]$	0.0007(3)	0.0002		
${}^2D_{5/2}8p [3/2]$	0.006(1)	0.002		
${}^2D_{5/2}5f [3/2, 1/2]$	0.0006(3)			
${}^2D_{5/2}9p [3/2]$	0.0030(6)	(0.0004)		
${}^2D_{5/2}6f [3/2, 1/2]$	0.00020(6)	(0.0004)		
${}^2D_{5/2}10p [3/2]$				
${}^2D_{3/2}7p [1/2]$	0.009(2)			
${}^2D_{5/2}7f [3/2, 1/2]$				

^aIncludes the $5s$ ionization channel only.

^bReference 4.

^cReference 2.

^dHartree-Fock calculation, Ref. 20.

^eIncludes the contribution from $5p5d^3D$ double-electron resonance.

TABLE V. Widths [full width at half maximum (FWHM)] of cadmium autoionizing resonances.

Peak	Width (meV)	
	This work	Absorption ^a
$^2D_{5/2}5p [3/2]$	38 ± 1	45
$^2D_{3/2}5p [1/2]$	145 ± 1^b	140
$^2D_{5/2}6p [3/2]$	7 ± 1	< 12
$^2D_{3/2}6p [1/2]$	6 ± 1	< 12
$^2D_{5/2}7p [3/2]$	5 ± 1	< 12
$^2D_{5/2}4f [3/2, 1/2]$	< 2	
$^2D_{3/2}8p [3/2]$	7 ± 1	< 12
$^2D_{5/2}5f [3/2, 1/2]$	< 1	
$^2D_{5/2}9p [3/2]$	5 ± 1	< 12
$^2D_{5/2}6f [3/2, 1/2]$	< 1	

^aReference 4.

^bTaken as the FWHM of the fitted peak (see text).

TABLE VI. Double-electron excitations.

Peak	State	Energy (eV)	Width (meV)	β
X_1	$5p6s \ ^1P$	11.861	25 ± 4	1.55
X_2	$5p5d \ ^3D$	12.856	15 ± 3	1.95
X_3	$5p5d \ ^1P$	13.237		1.95
X_4	$5p7s \ ^3P$	13.297	16 ± 3	1.61

Our cross section at the peak of the first resonance (12.063 eV) is 65% of the result of Marr and Austin.⁴ This might be due in part to the fact that this resonance is closer to threshold, and our detection efficiency, which decreases toward the low kinetic energies, might have decreased more rapidly than we determined with the Xe 5p calibration lines. The other resonances studied in this work are in a region of constant detection efficiency.

In the original work by Beutler,¹ the first resonance at 12.063 eV was labeled as $4d^9 5s^2 5p \ ^1P$, and the second resonance at 12.805 eV as $4d^9 5s^2 5p \ ^3P$. This notation has been used in experimental work in cadmium since that time. On the other hand, in the calculations of Wilson²⁰ and Martin *et al.*¹⁸ it is shown that there is a strong mixing of the states within this configuration, and that the main contribution to the low-energy resonance comes from a 3P state while the second resonance is predominantly a 1P state. From Eq. (4) and our results for β one can see that the coupling to the triplet continuum is strongest in the vicinity of the first resonance. Therefore the correct assignment for this line is 3P . On the other hand, $\beta=2$ across the resonance at 12.805 eV, so this peak corresponds to the production of a 1P state. This assignment and the measured spacings of the lines in this configuration are in good accord with the results of Wilson,²⁰ Martin *et al.*,¹⁸ and Mansfield and Murnane.²¹ There is overall agreement between our data and the semiempirical calculation of Martin²² for β , except that the experimental dips are broader because of resolution.

In the variation of β there is also an indication of the presence of several states produced by the simultaneous excitation of both 5s electrons (X_1 - X_4). We studied the double-electron resonances in the vicinity of the 5p lines. In all cases, except for the $5p5d \ ^3D_1$ resonance discussed below, we used the assignments of Mansfield and Murnane²¹ for these states. The parameters of these lines are presented in Table VI. The $5p6s \ ^1P$ and $5p7s \ ^3P$ appear as window resonances, while the shape of the $5p5d \ ^1P$ peak is asymmetric.

The optically allowed transition X_2 can be seen as a shoulder on the 1P main line and a dip in the value of β . To obtain more information about this peak a Lorentzian profile was fitted to the low-energy half of the 1P resonance and folded over onto the high-energy side. The difference between this fitted line and the data is shown in Fig. 4: the "complete" $5p \ ^1P$ Lorentzian is displayed in the lower panel and the result of the subtraction is presented in the top portion. In addition to the Fano-shaped $4d^9 5s^2 5p \ ^3D$ line at 12.938 eV there is a strong "window" resonance for the peak X_2 at 12.856 eV. This peak has also been observed in electron-impact measurements.^{11,12} Mansfield and Murnane²¹ assigned this line

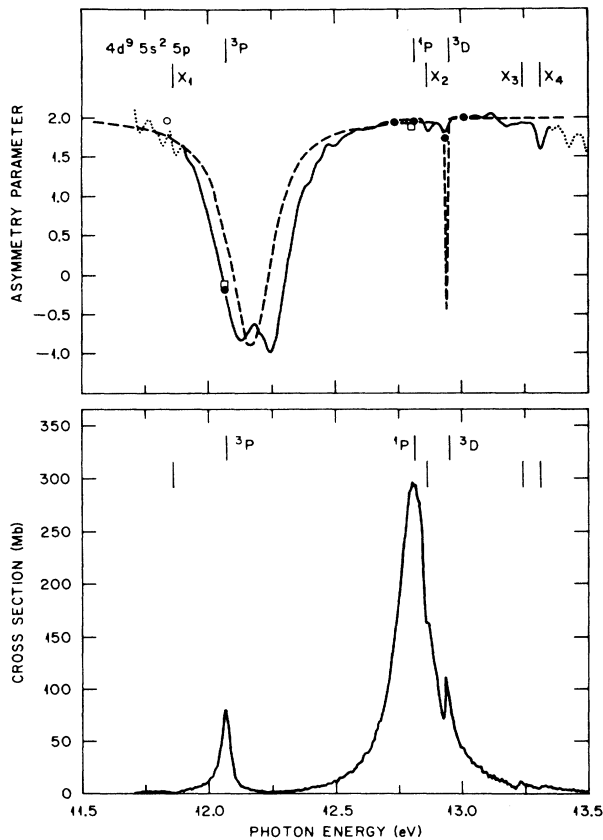


FIG. 3. Angular distribution parameter β (upper panel) and cross section σ (lower panel) of the 5s photoelectron in the region of the $4d \rightarrow 5p$ resonances. These data were obtained in the CIS mode using 3-meV increments; data are fully corrected. \circ , β value from photoionization (Ref. 6); \square , electron-impact excitation results (Ref. 22). — — —, semiempirical calculation (Ref. 22); \bullet , reference values obtained from PES spectra. indicates a region where poor statistics did not allow an accurate determination of β . The two-electron excitations X_1 to X_4 are identified in Table VI.

incorrectly to the $5p5d\ ^1F_2$ state. We agree with Pejcev *et al.*¹² on the basis of a quantum defect analysis, in that this line corresponds to a transition to the $5p5d\ ^3D_1$ state. By taking the limit of the $5pnd\ ^3D_1$ series at 14.466 eV,⁵ we calculate a quantum defect of 2.093 for this $5p5d\ ^3D$ resonance, in good agreement with the results obtained for the higher resonances.⁵

The fit was also used to calculate the oscillator strength of the $5p[1/2]$ resonance given in Table IV. By subtracting this f value from that obtained by considering the area under the experimental peak we were able to obtain the combined oscillator strength of the $^2D_{3/2}5p[3/2]$ and $5p5d\ ^3D_1$ resonances shown in Table IV.

B. $4d^95s^26p$ resonances

The $6p$ resonances are displayed in Fig. 5. In this case the values of the angular distribution parameter β are neither near -1 nor near 2 at the resonances, indicating that there is a stronger mixing of singlet and triplet states within this configuration. Nevertheless, it is clear that there is an inversion with respect to the $5p$ resonances in the relative position of the line with stronger singlet com-

ponent and the line with stronger triplet contribution. Here II coupling seems to be more adequate and this condition should prevail at the higher resonances according to Martin *et al.*¹⁸

The sharp excursion in β at 16.09 eV seems to indicate the presence of a peak. A more detailed study of the cross-section spectrum in this region reveals a weak resonance shown in the lower panel of Fig. 5. This line has not been seen previously, and we tentatively assign it to the state $4d^95s5d\ ^1P$. It peaks at 16.112 eV, with an absolute cross section of 2.0 ± 0.6 Mb. Its width is 13 meV.

C. Other resonances below the $^2D_{5/2}$ ionic threshold

The $\text{Cd}^+ 4d^95s^2D_{5/2}$ threshold is at 17.581 eV. Below this energy there is just one more line of the series converging to the $D_{3/2}$ ionic state, namely, the $7p[1/2]$ resonance. All the other lines belong to the $4d^95s^2(^2D_{5/2})np, nf$ series. In Fig. 6 we present the results obtained for the cross section and the asymmetry parameter β in this region. The β value of the nf resonances does not change very much, while it tends to decrease with n for the $np[3/2]$ lines just below the $7p[1/2]$ line. Closer to the limit it is impossible to distinguish in-

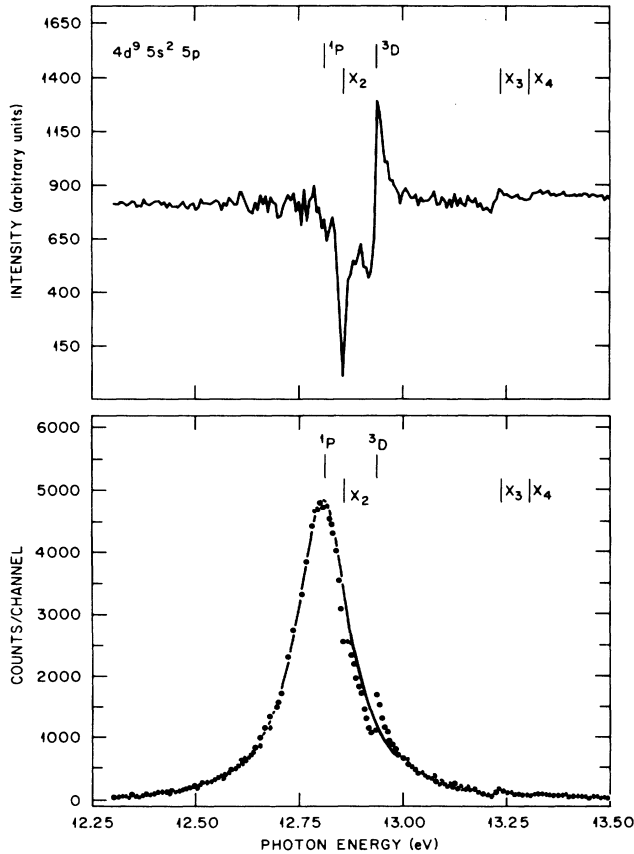


FIG. 4. $5p5d\ ^1P$ resonance. Lower panel shows the experimental data (closed circle) and the Lorentzian fit (solid line) based on the low-energy side of peak. Upper panel shows the difference between the fit and the experimental data. The peak position of the $5p\ ^1P$ resonance is also indicated in the upper panel. The two-electron resonances are identified in Table VI.

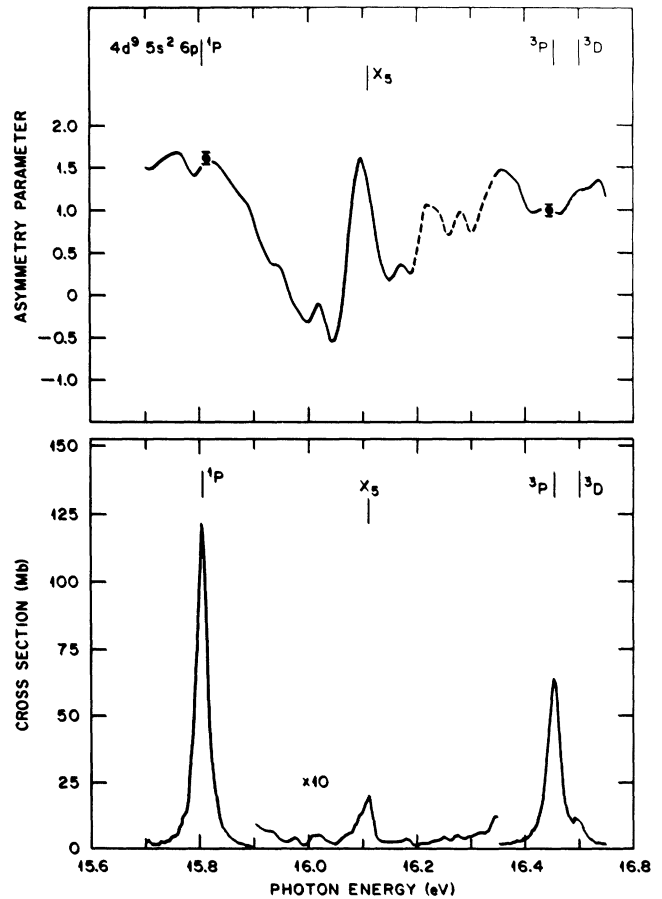


FIG. 5. Angular distribution parameter β (upper panel) and cross section σ (lower panel) of the $5s$ photoelectron in the region of the $4d \rightarrow 6p$ resonances. ●, reference PES values, — — — indicates a region of poor statistics.

dividual lines, and the value of the asymmetry parameter is high again, until it drops at the ${}^2D_{5/2}$ ionic limit.

D. Resonances between the ${}^2D_{5/2}$ and ${}^2D_{3/2}$ thresholds

Our results in the interval between the 2D_J thresholds are shown in Fig. 7. Here we only have the np and nf series. The β values at the np lines are consistently lower, and they tend to slowly increase. On the other hand, at the nf peaks, $\beta=1.75$ and remains almost constant. This value is very close to that of the ${}^2D_{5/2}nf$ resonances.

This region of the spectrum is the same as that explored in detail in the alignment measurements of Goodman, Caldwell, and White.¹⁰ Because of the weaker direct contribution, we were able to isolate the $5f$ resonance more completely from the $8p$ resonance than they were able to. The fact that the direct $5s$ channel is so weak is evident in comparing the line shapes of the $8p$ peaks. Ours is quite symmetric, whereas theirs is strongly asymmetric on the low-energy side. While it is perhaps not appropriate to compare β values and alignment measurements for decay into two different final ionic states, we do observe that our β values differ considerably for the $8p$ and $5f$ transitions. This is in contrast to the alignment results, which were comparable for both.

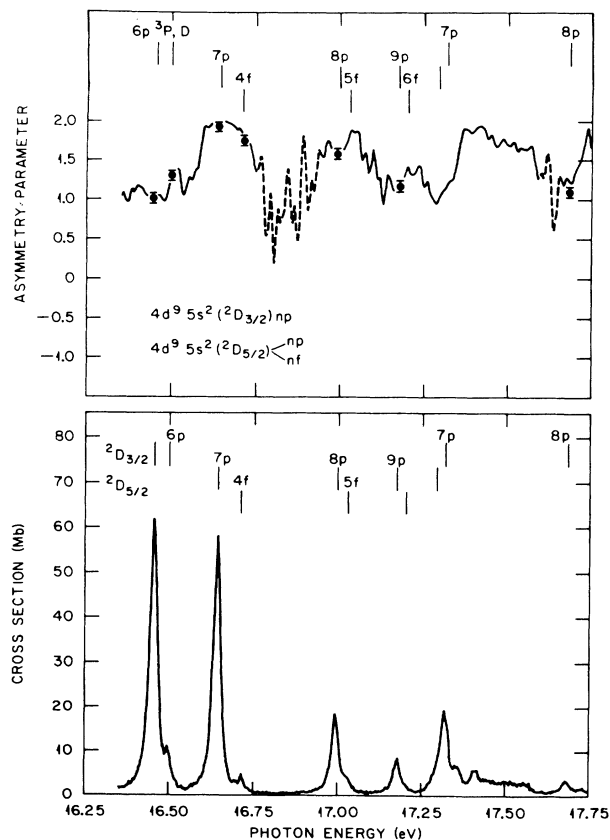


FIG. 6. Asymmetry parameter β (upper panel) and cross section σ (lower panel) for the $5s$ photoelectron in the region just below the $\text{Cd}^+(4d^9 5s^2 {}^2D_{3/2})$ threshold at 17.58 eV. ●, reference PES values; — — is a region of poor statistics.

IV. CONCLUSIONS

In this electron spectrometry study of cadmium we measured the relative cross section and the angular distribution parameter of the $5s$ photoelectrons in the region of the $4d \rightarrow nl$ autoionizing resonances. The results for the resonance energies are in good agreement with the data from other experiments. Our oscillator strengths are higher than the values measured by other groups but are in good accord with theoretical calculations. There is also good agreement with the semiempirical calculation for β by Martin²² in the region of the $4d \rightarrow 5p$ resonances.

This work illustrates the usefulness of the angular distribution measurements. The value of the angular distribution parameter allowed us to unambiguously determine the singlet or triplet nature of the autoionizing peaks. Changes in the β values also enabled us to detect a previously unobserved line.

Theoretical results are needed for both cross sections and asymmetry parameters, especially at the higher resonances. Also needed are measurements of β for the $4d_{5/2}$ photoelectron between the 2D_J thresholds. This would provide information complementary to the alignment results of Goodman *et al.*¹⁰ From examination of the same ionic state one might hope to determine the relative

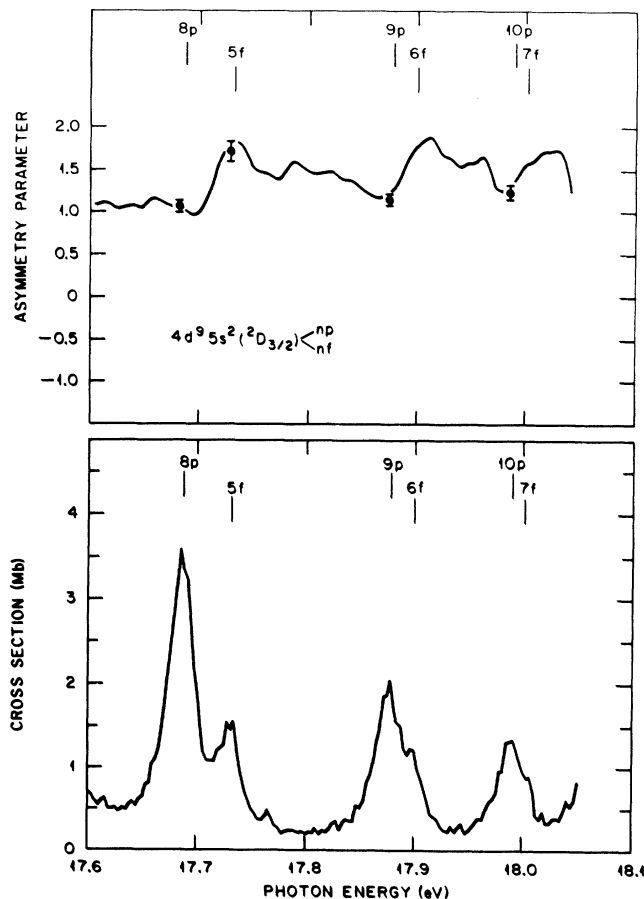


FIG. 7. Angular distribution parameter β (upper panel) and cross section σ (lower panel) for the $5s$ photoelectron in the region between the ${}^2D_{5/2}$ and ${}^2D_{3/2}$ ionic thresholds showing the $4d^9 5s^2 {}^2D_{3/2} np, nf$ resonance series. ●, reference PES values.

phase shifts and absolute probability amplitudes of the different exit channels. Finally, the behavior of the $5p\ ^2P$ channel remains to be studied in detail through the autoionization resonance structure.

ACKNOWLEDGMENTS

This work was sponsored by the Division of Chemical Sciences, Office of Basic Energy Sciences, U.S. Depart-

ment of Energy under Contract No. DE-AC05-84OR21400 with Martin Marietta Energy Systems, Inc. One of us (C.D.C.) was supported by the National Science Foundation (NSF) under Grant Nos. NSF-PHY-8701193 and NSF-PHY-8707550 and acknowledges travel support from the Oak Ridge Associated Universities. The University of Wisconsin Synchrotron Radiation Center is operated under NSF Grant No. DMR-8601349.

*Permanent address: Instituto de Ciencias Nucleares, Universidad Nacional Autónoma de México, México 04510, D.F. México.

¹H. Beutler, *Z. Phys.* **87**, 19 (1933).

²J. Berkowitz and C. Lifshitz, *J. Phys. B* **1**, 438 (1968).

³W. R. S. Garton and J. P. Connerade, *Astrophys. J.* **155**, 667 (1969).

⁴G. V. Marr and J. M. Austin, *Proc. R. Soc. London, Ser. A* **310**, 137 (1969).

⁵M. W. D. Mansfield, *Proc. R. Soc. London, Ser. A* **362**, 129 (1978).

⁶H. Harrison, *J. Chem. Phys.* **52**, 901 (1970).

⁷C. D. Caldwell and R. N. Zare, *Phys. Rev. A* **16**, 255 (1977).

⁸P. Kobrin, J. Becker, S. Southworth, C. M. Truesdale, D. W. Lindle, and D. A. Shirley, *Phys. Rev. A* **26**, 842 (1982).

⁹W. Kronast, R. Huster, and W. Mehlhorn, *Z. Phys. D* **2**, 285 (1986).

¹⁰Z. M. Goodman, C. D. Caldwell, and M. G. White, *Phys. Rev. Lett.* **54**, 1156 (1985).

¹¹V. Pejcev, K. J. Ross, D. Rassi, and T. W. Ottley, *J. Phys. B*

10, 459 (1977).

¹²V. Pejcev, D. Rassi, and K. J. Ross, *J. Phys. B* **10**, L629 (1977).

¹³N. L. S. Martin, T. W. Ottley, and K. J. Ross, *J. Phys. B* **13**, 1867 (1980).

¹⁴N. L. S. Martin and K. J. Ross, *J. Phys. B* **17**, 4033 (1984).

¹⁵S. Süzer, S.-T. Lee, and D. A. Shirley, *Phys. Rev. A* **13**, 1842 (1976).

¹⁶M. O. Krause, T. A. Carlson, and P. R. Woodruff, *Phys. Rev. A* **24**, 1374 (1981).

¹⁷M. O. Krause, T. A. Carlson, and A. Fahlman, *Phys. Rev. A* **30**, 1316 (1984).

¹⁸W. C. Martin, J. Sugar, and J. L. Tech, *J. Opt. Soc. Am.* **62**, 1488 (1972).

¹⁹D. Dill, *Phys. Rev. A* **7**, 1976 (1973)

²⁰M. Wilson, *J. Phys. B* **1**, 736 (1968).

²¹M. W. D. Mansfield and M. M. Murnane, *J. Phys. B* **18**, 4223 (1985).

²²N. L. S. Martin, *Bull. Am. Phys. Soc.* **31**, 936 (1986); (private communication).